CRYSTALLOGRAPHIC
COMMUNICATIONS

ISSN 2056-9890

Received 23 April 2025
Accepted 16 May 2025

Edited by F. F. Ferreira, Universidade Federal do ABC, Brazil

Keywords: pyrene Schiff base; Hirshfeld surface; energy framework analysis; hydrogen bond; π-stacking; crystal structure.

CCDC reference: 2452369

Supporting information: this article has supporting information at journals.iucr.org/e

Crystal structure and Hirshfeld surface analyses, crystal voids, interaction energy calculations and energy frameworks of (*E*)-2-[(pyren-1-ylmethylidene)amino]ethanol

Naser E. Eltayeb,[a,b]* Tuncer Hökelek[c] and Jamal Lasri[a]

[a]Department of Chemistry, Rabigh College of Science and Arts, King Abdulaziz University, Jeddah 21589, Saudi Arabia, [b]Department of Chemistry, Faculty of Pure and Applied Sciences, International University of Africa, Khartoum 2469, Sudan, and [c]Department of Physics, Hacettepe University, 06800 Beytepe, Ankara, Türkiye. *Correspondence e-mail: netaha@kau.edu.sa

The title compound, $C_{19}H_{15}NO$, contains a pyrene ring system, consisting of four fused benzene rings arranged in a planar configuration. In the crystal, intermolecular O—H···N hydrogen bonds link the molecules into infinite chains along the *c*-axis direction. π–π stacking interactions between the benzene rings of adjacent molecules help to consolidate the three-dimensional architecture. A Hirshfeld surface analysis indicates that the most important contributions for the crystal packing are from H···H (56.4%), H···C/C···H (16.6%) and C···C (15.8%) interactions. The volume of the crystal voids and the percentage of free space were calculated to be 76.07 Å^3 and 5.79%, showing that there is no large cavity in the crystal packing. An evaluation of the electrostatic, dispersion and total energy frameworks indicates that the dispersion energy contribution is dominant while hydrogen bonding, $\pi\cdots\pi$ and van der Waals interactions are the dominant interactions in the crystal packing.

1. Chemical context

Schiff bases have garnered significant attention in coordination and medicinal chemistry and in materials science due to their structural versatilities, ease of syntheses, and diverse applications (Gupta & Sutar, 2008). The abilities of Schiff bases to act as chelating ligands by coordinating various transition-metal ions make them valuable in catalysis, bioorganic chemistry, and in the development of metallodrugs (da Silva *et al.*, 2011). Additionally, their biological activities including antimicrobial (Malik *et al.*, 2018) and antioxidant properties (Kumar *et al.*, 2017) have made them promising candidates for pharmaceutical applications. Schiff bases also find utility in industrial processes such as corrosion inhibition (Omar *et al.*, 1986), polymer stabilization (Sabaa *et al.*, 2009), and as sensors for metal ion detection (Alam *et al.*, 2023). Currently, our research program focuses on the syntheses and evaluations of anticancer activities of Schiff base type compounds (Lasri *et al.*, 2018, 2023*a*,*b*, 2024; Eltayeb *et al.*, 2020*a*,*b*). Herein, we report the synthesis, molecular and crystal structures, Hirshfeld surface analysis, crystal voids, interaction energies and energy frameworks of the title compound (I).

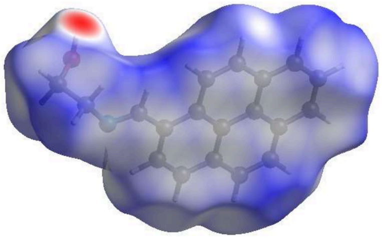

2. Structural commentary

The title compound contains a planar pyrene ring system, consisting of four fused benzene rings [*A* (C4–C17/C18), *B*

https://doi.org/10.1107/S2056989025004451

(C7–C10/C18/C19), *C* (C10–C14/C19) and *D* (C14–C19)] arranged in a planar configuration (Fig. 1), where atom C3 is 0.0255 (13) Å away from the best least-squares plane of the ring system. The C2—N1—C3—C4, N1—C3—C4—C5, N1—C3—C4—C17 and O1—C1—C2—N1 torsion angles are −178.71 (11), −9.67 (19), 171.23 (12) and −61.54 (14)°, respectively. There are no unusual bond distances or interbond angles in the molecule.

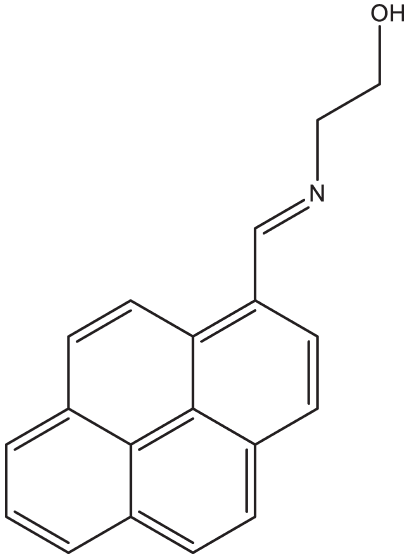

3. Supramolecular features

In the crystal, intermolecular O—H···N hydrogen bonds (Table 1) link the molecules into infinite chains along the *c*-axis direction (Fig. 2). π–π stacking interactions occur between the benzene rings of adjacent molecules with the inter-centroid distances of 4.3657 (18) Å [between *A* rings, α = 0.02 (6)° and slippage = 2.632], 3.6343 (16) Å [between *A* and *B* rings, α = 0.05 (6)° and slippage = 1.079], 3.7953 (16) Å [between *A* and *C* rings, α = 1.90 (6)° and slippage = 1.663], 3.6538 (16) Å [between *A* and *D* rings, α = 1.10 (6)° and slippage = 1.418], 4.4161 (18) Å [between *B* rings, α = 0.00 (6)° and slippage = 2.727], 3.8279 (16) Å [between *B* and *D* rings, α = 0.14 (6)° and slippage = 1.609], 4.1054 (17) Å [between *D* rings, α = 0.00 (6)° and slippage = 2.367] and may help to consolidate the three-dimensional architecture. No C—H···π(ring) interactions are identified.

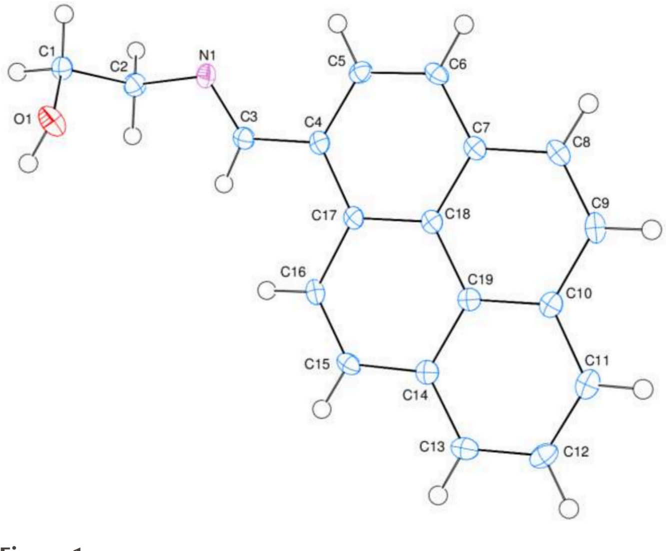

Figure 1
The title molecule with atom-numbering scheme and 50% probability ellipsoids.

Table 1
Hydrogen-bond geometry (Å, °).

D—H···*A*	*D*—H	H···*A*	*D*···*A*	*D*—H···*A*
O1—H1···N1^{i}	0.853 (17)	1.997 (16)	2.8440 (18)	171.6 (14)

Symmetry code: (i) $x, -y+\frac{1}{2}, z+\frac{1}{2}$.

Table 2
Selected interatomic distances (Å).

O1···N1	2.9300 (19)	H1···C2^{i}	2.841 (16)
O1···N1^{i}	2.8440 (18)	C3···H16	2.65
N1···H5	2.62	C16···H3	2.63
H1···N1^{i}	1.997 (16)	H1···H5^{i}	2.33
C3···C19^{ii}	3.386 (2)	H2*A*···H3	2.07
C17···C17^{ii}	3.396 (2)	H3···H16	2.06

Symmetry codes: (i) $x, -y+\frac{1}{2}, z+\frac{1}{2}$; (ii) $-x+1, -y+1, -z+1$.

4. Hirshfeld surface analysis

A Hirshfeld surface (HS) analysis (Hirshfeld, 1977; Spackman & Jayatilaka, 2009) was carried out using *Crystal Explorer 17.5* (Spackman *et al.*, 2021) to clarify the intermolecular interactions (Table 2) in the crystal of the title compound (I). The contact distances (Table 2) (Venkatesan *et al.*, 2016) are shown in Fig. 3, where the bright-red spots correspond to the respective donors and/or acceptors; they also appear as blue and red regions in Fig. 4 corresponding to positive and negative potentials (Spackman *et al.*, 2008; Jayatilaka *et al.*, 2005). Fig. 5 shows only the presence of the π–π interactions in

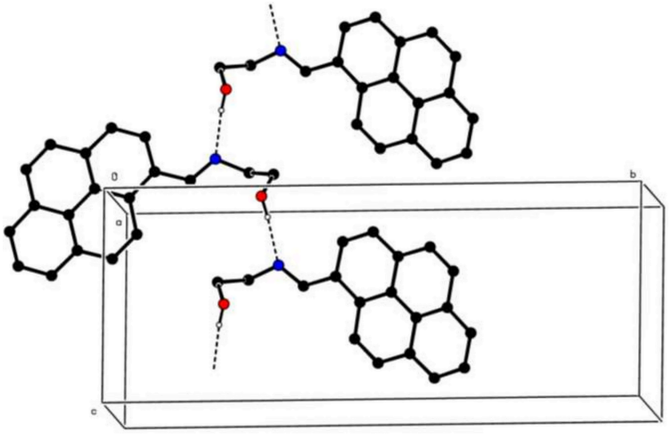

Figure 2
A partial packing diagram viewed down the *a*-axis direction. Intermolecular O—H···N hydrogen bonds are shown as dashed lines. H atoms not involved in these interactions have been omitted for clarity.

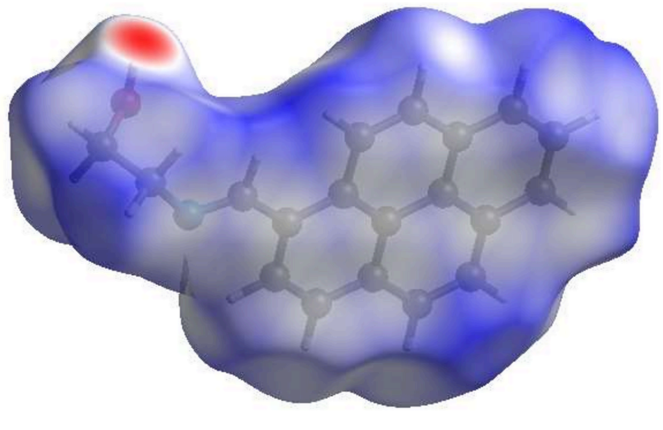

Figure 3
View of the three-dimensional Hirshfeld surface of the title compound plotted over $d_{\rm norm}$.

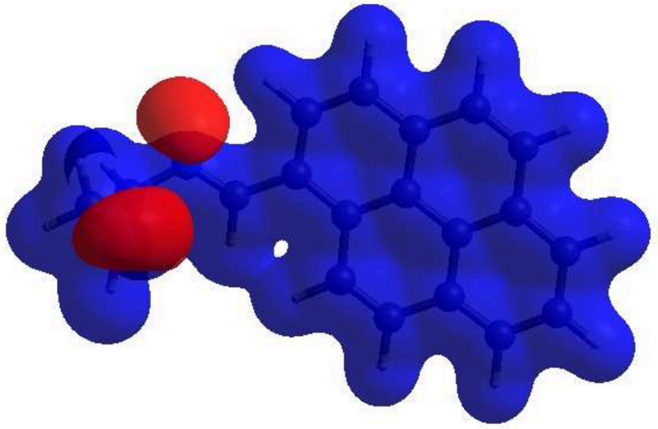

Figure 4
View of the Hirshfeld surface of the title compound plotted over electrostatic potential energy in the range of −0.0500 to 0.0500 a.u. using the STO-3 G basis set at the Hartree–Fock level of theory. Hydrogen-bond donors and acceptors are shown as blue and red regions around the atoms corresponding to positive and negative potentials, respectively.

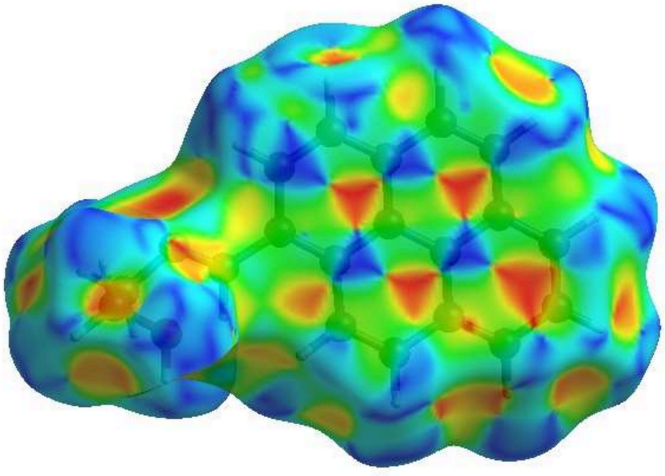

Figure 5
Hirshfeld surface of the title compound plotted over shape-index.

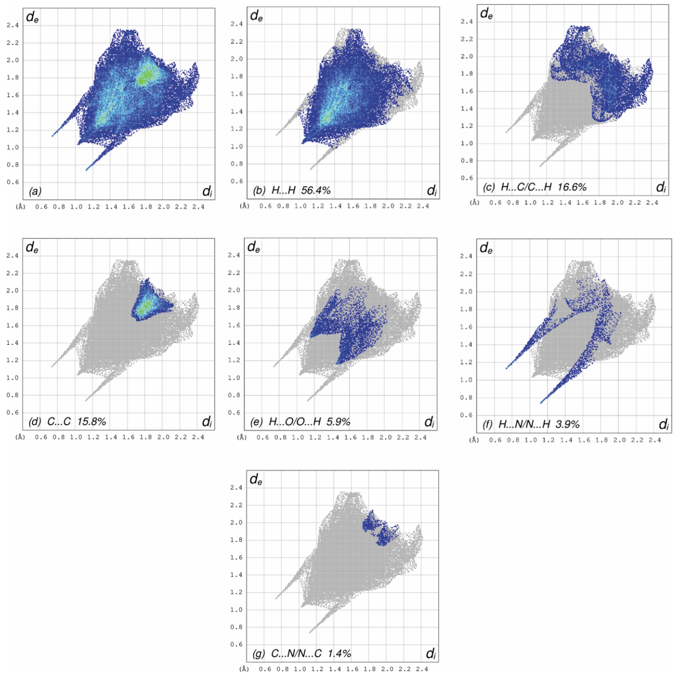

Figure 6
The full two-dimensional fingerprint plots for the title compound, showing (*a*) all interactions, and delineated into (*b*) H···H, (*c*) H···C/C···H, (*d*) C···C, (*e*) H···O/O···H, (*f*) H···N/N···H and (*g*) C···N/N···C, interactions. The d_i and d_e values are the closest internal and external distances (in Å) from given points on the Hirshfeld surface contacts.

(I). According to the 2D fingerprint plots (McKinnon *et al.*, 2007), the intermolecular H···H (Table 2), H···C/C···H and C···C (Table 2) contacts make important contributions to the HS of 56.4%, 16.6% and 15.8%, respectively (Fig. 6). Their contact patches are also plotted onto the surface as shown in Fig. 7, suggesting that van der Waals interactions and hydrogen bonding play the major roles in the crystal packing (Hathwar *et al.*, 2015).

5. Crystal voids

If the molecules are tightly packed and an applied external mechanical force does not easily break the crystal, then the crystal packing does not result in significant voids. A void analysis was performed by adding up the electron densities of the spherically symmetric atoms contained in the asymmetric unit (Turner *et al.*, 2011). The volume of the crystal voids (Fig. 8) and the percentage of free space in the unit cell are

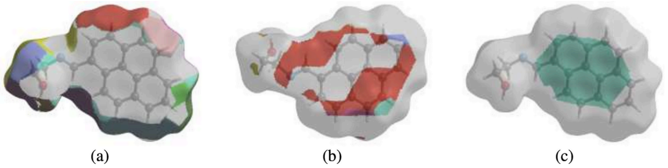

Figure 7
The Hirshfeld surface representations of contact patches plotted onto the surface for (*a*) H···H, (*b*) H···C/C···H and (*c*) C···C interactions.

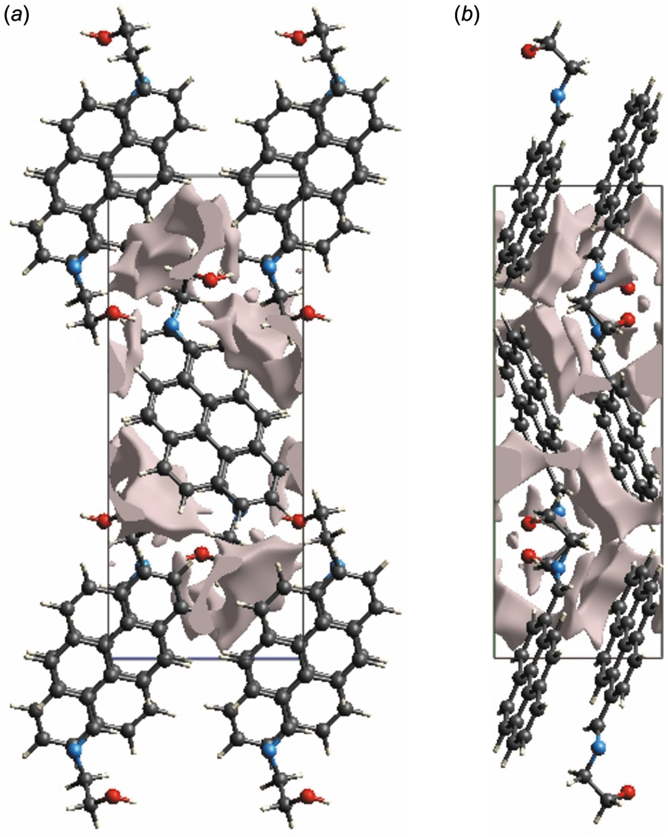

Figure 8
Graphical views of voids in the crystal packing of the title compound along the (*a*) *a*-axis and (*b*) *c*-axis directions.>

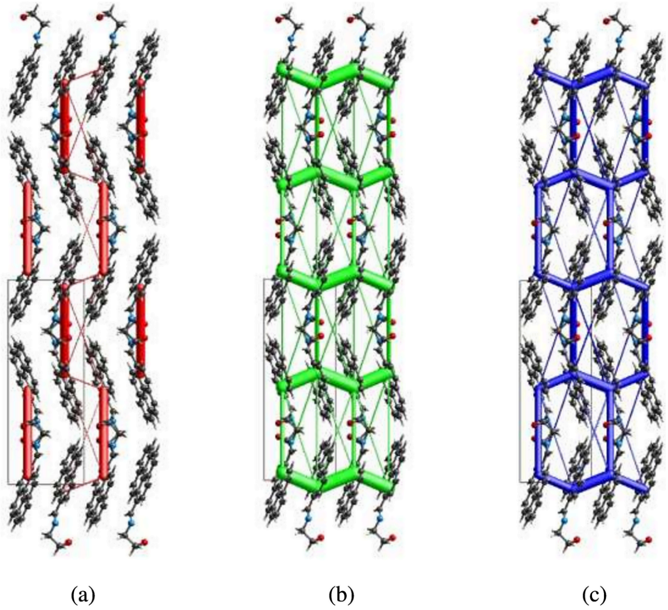
(a)
(b)
(c)

Figure 9
The energy frameworks for a cluster of molecules of the title compound viewed down the *c*-axis showing the (*a*) electrostatic energy, (*b*) dispersion energy and (*c*) total energy diagrams. The cylindrical radius is proportional to the relative strength of the corresponding energies and they were adjusted to the same scale factor of 80 with cut-off value of 5 kJ mol^{-1} within 2 × 2 *X* 2 unit cells.

Table 3
Experimental details.

Crystal data	
Chemical formula	$C_{19}H_{15}NO$
M_r	273.32
Crystal system, space group	Monoclinic, $P2_1/c$
Temperature (K)	100
a, b, c (Å)	7.447 (2), 20.916 (8), 8.446 (3)
β (°)	93.347 (9)
V (Å^3)	1313.3 (8)
Z	4
Radiation type	Mo *Kα*
μ (mm^{-1})	0.09
Crystal size (mm)	0.37 × 0.35 × 0.28
Data collection	
Diffractometer	Bruker D8 Quest
Absorption correction	Multi-scan (*SADABS*; Krause *et al.*, 2015)
No. of measured, independent and observed [$I > 2\sigma(I)$] reflections	14470, 2362, 1980
$R_{\rm int}$	0.044
$(\sin \theta/\lambda)_{\rm max}$ (Å^{-1})	0.601
Refinement	
$R[F^2 > 2\sigma(F^2)]$, $wR(F^2)$, S	0.038, 0.106, 1.04
No. of reflections	2362
No. of parameters	193
H-atom treatment	H atoms treated by a mixture of independent and constrained refinement
$\Delta\rho_{\rm max}$, $\Delta\rho_{\rm min}$ (e Å^{-3})	0.18, −0.25

Computer programs: *APEX3* and *SAINT* (Bruker, 2021), *SHELXT2014/5* (Sheldrick, 2015*a*), *SHELXL2018/3* (Sheldrick, 2015*b*) and *SHELXTL* (Sheldrick, 2008).

calculated as 76.07 Å^3 and 5.79%, respectively, indicating that the crystal packing is compact.

6. Interaction energy calculations and energy frameworks

The CE–B3LYP/6–31G(d,p) energy model available in *Crystal Explorer 17.5* (Spackman *et al.*, 2021) was used to calculate the intermolecular interaction energies. Hydrogen-bonding interaction energies (in kJ mol^{-1}) were calculated to be −9.8 ($E_{\rm ele}$), −14.2 ($E_{\rm pol}$), −103.3 ($E_{\rm dis}$), 52.1 ($E_{\rm rep}$) and −70.0 ($E_{\rm tot}$) for O1—H1···N1. Energy frameworks combine the calculation of intermolecular interaction energies with a graphical representation of their magnitude (Turner *et al.*, 2015). Energy frameworks were constructed for $E_{\rm ele}$ (red cylinders), $E_{\rm dis}$ (green cylinders) and $E_{\rm tot}$ (blue cylinders) (Fig. 9*a*, *b* and *c*), and their evaluation indicates that the stabilization is dominated *via* the dispersion energy contributions in the crystal structure of (I).

7. Synthesis and crystallization

To a solution of 1-pyrenecarboxaldehyde (0.230 g, 1.0 mmol) in ethanol (25 ml) was added 2-aminoethanol (0.073 g, 1.2 mmol) and the reaction mixture was refluxed for 4 h. The reaction mixture was cooled down to room temperature for precipitation, and then filtered. The precipitate was washed with cold ethanol and dried in air. Yellow crystals suitable for X-ray analysis were obtained by slow evaporation of an ethanol solution. Yield: 80%. FT–IR (cm^{-1}): 3440 (OH), 1631 (C═N), 1594 (C═C). ^{1}H NMR (CDCl$_3$): 9.34 (*s*, 1H, N═CH), 9.12 (*d*, 1H, $J_{\rm H–H}$ = 9.6 Hz, pyrenyl), 8.56 (*d*, 1H, $J_{\rm H–H}$ = 7.8 Hz, pyrenyl), 8.36 (*m*, 7H, pyrenyl), 4.73 (*t*, $J_{\rm H–H}$ = 5.4 Hz, OH), 3.87 (*dd*, 4H, $J_{\rm H–H}$ = 4.8 and 5.4 Hz, CH$_2$). ^{13}C NMR (CDCl$_3$): 161.83, 131.23, 128.75, 128.68, 127.41, 126.21, 125.97, 125.70, 124.92, 122.38, 64.20, 62.70; HRMS: *m*/*z*: 273.11 [M]$^+$. Analysis calculated (%) for $C_{19}H_{15}NO$: C 83.49, H 5.53, N 5.12; found C 83.47, H 5.51, N 5.10.

8. Refinement

Crystal data, data collection and structure refinement details are summarized in Table 3. The OH hydrogen atom was located in a difference-Fourier map, and refined isotropically. The C-bound hydrogen-atom positions were calculated geometrically at distances of 0.93 Å (for aromatic CH) and 0.97 Å (for CH$_2$) and refined using a riding model by applying the constraint $U_{\rm iso}$(H) = 1.2$U_{\rm eq}$(C).

Funding information

TH is grateful to Hacettepe University Scientific Research Project Unit (grant No. 013 D04 602 004).

References

Alam, M. Z., Alimuddin & Khan, S. A. (2023). *J. Fluoresc.* **33**, 1241–1272.

Bruker (2021). *APEX3* and *SAINT*. Bruker AXS Inc, Madison, Wisconsin, USA.

da Silva, C. M., da Silva, D. L., Modolo, L. V., Alves, R. B., de Resende, M. A., Martins, C. V. B. & de Fátima, Á. (2011). *J. Adv. Res.* **2**, 1–8.

Eltayeb, N. E., Lasri, J., Soliman, S. M., Mavromatis, C., Hajjar, D., Elsilk, S. E., Babgi, B. A. & Hussien, M. A. (2020*b*). *J. Mol. Struct.* **1213**, 128185.

Eltayeb, N. E., Şen, F., Lasri, J., Hussien, M. A., Elsilk, S. E., Babgi, B. A., Gökçe, H. & Sert, Y. (2020*a*). *J. Mol. Struct.* **1202**, 127315.

Gupta, K. C. & Sutar, A. K. (2008). *Coord. Chem. Rev.* **252**, 1420–1450.

Hathwar, V. R., Sist, M., Jørgensen, M. R. V., Mamakhel, A. H., Wang, X., Hoffmann, C. M., Sugimoto, K., Overgaard, J. & Iversen, B. B. (2015). *IUCrJ*, **2**, 563–574.

Hirshfeld, H. L. (1977). *Theor. Chim. Acta* **44**, 129–138.

Jayatilaka, D., Grimwood, D. J., Lee, A., Lemay, A., Russel, A. J., Taylor, C., Wolff, S. K., Cassam-Chenai, P. & Whitton, A. (2005). *TONTO* - A System for Computational Chemistry. Available at: http://hirshfeldsurface.net/

Krause, L., Herbst-Irmer, R., Sheldrick, G. M. & Stalke, D. (2015). *J. Appl. Cryst.* **48**, 3–10.

Kumar, M., Padmini, T. & Ponnuvel, K. (2017). *J. Saudi Chem. Soc.* **21**, S322–S328.

Lasri, J., Elsherbiny, A. S., Eltayeb, N. E., Haukka, M. & El-Hefnawy, M. E. (2018). *J. Organomet. Chem.* **866**, 21–26.

Lasri, J., Eltayeb, N. E., Soliman, S. M., Ali, E. M. M., Alhayyani, S. & Akhdhar, A. (2023*a*). *Molecules* **28**, 4766.

Lasri, J., Eltayeb, N. E., Soliman, S. M., Ali, E. M. M., Alhayyani, S., Akhdhar, A. & Hussien, M. A. (2023*b*). *J. Mol. Struct.* **1287**, 135673.

Lasri, J., Eltayeb, N. E., Soliman, S. M., Ali, E. M. M., Rosli, M. M., Alzahrani, F. A., Eid, T. M., Alhayyani, S., Akhdhar, A., Dutta, A., Jaremko, M., Emwas, A. H. & Almaqwashi, A. A. (2024). *ChemistrySelect* **9**, e202402236.

Malik, M. A., Dar, O. A., Gull, P., Wani, M. Y. & Hashmi, A. A. (2018). *Med. Chem. Commun.* **9**, 409–436.

McKinnon, J. J., Jayatilaka, D. & Spackman, M. A. (2007). *Chem. Commun.* pp. 3814–3816.

Omar, I. H., Zucchi, F. & Trabanelli, G. (1986). *Surf. Coat. Technol.* **29**, 141–151.

Sabaa, M. W., Mohamed, R. R. & Oraby, E. H. (2009). *Eur. Polym. J.* **45**, 3072–3080.

Sheldrick, G. M. (2008). *Acta Cryst.* A**64**, 112–122.

Sheldrick, G. M. (2015*a*). *Acta Cryst.* A**71**, 3–8.

Sheldrick, G. M. (2015*b*). *Acta Cryst.* C**71**, 3–8.

Spackman, M. A. & Jayatilaka, D. (2009). *CrystEngComm* **11**, 19–32.

Spackman, M. A., McKinnon, J. J. & Jayatilaka, D. (2008). *CrystEngComm.* **10**, 377–388.

Spackman, P. R., Turner, M. J., McKinnon, J. J., Wolff, S. K., Grimwood, D. J., Jayatilaka, D. & Spackman, M. A. (2021). *J. Appl. Cryst.* **54**, 1006–1011.

Turner, M. J., McKinnon, J. J., Jayatilaka, D. & Spackman, M. A. (2011). *CrystEngComm* **13**, 1804–1813.

Turner, M. J., Thomas, S. P., Shi, M. W., Jayatilaka, D. & Spackman, M. A. (2015). *Chem. Commun.* **51**, 3735–3738.

Venkatesan, P., Thamotharan, S., Ilangovan, A., Liang, H. & Sundius, T. (2016). *Spectrochim. Acta A Mol. Biomol. Spectrosc.* **153**, 625–636.

supporting information

Acta Cryst. (2025). E**81**, 595-599   [https://doi.org/10.1107/S2056989025004451]

Crystal structure and Hirshfeld surface analyses, crystal voids, interaction energy calculations and energy frameworks of (*E*)-2-[(pyren-1-ylmethylidene)amino]ethanol

Naser E. Eltayeb, Tuncer Hökelek and Jamal Lasri

Computing details

(*E*)-2-[(Pyren-1-ylmethylidene)amino]ethanol

Crystal data

$C_{19}H_{15}NO$
$M_r = 273.32$
Monoclinic, $P2_1/c$
$a = 7.447$ (2) Å
$b = 20.916$ (8) Å
$c = 8.446$ (3) Å
$\beta = 93.347$ (9)°
$V = 1313.3$ (8) Å^3
$Z = 4$

$F(000) = 576$
$D_x = 1.382$ Mg m^{-3}
Mo $K\alpha$ radiation, $\lambda = 0.71073$ Å
Cell parameters from 7593 reflections
$\theta = 2.6$–25.4°
$\mu = 0.09$ mm^{-1}
$T = 100$ K
Block, colourless
0.37 × 0.35 × 0.28 mm

Data collection

Bruker D8 Quest diffractometer
φ and ω scans
Absorption correction: multi-scan (SADABS; Krause *et al.*, 2015)

14470 measured reflections

2362 independent reflections
1980 reflections with $I > 2\sigma(I)$
$R_{\text{int}} = 0.044$
$\theta_{\max} = 25.3°$, $\theta_{\min} = 2.7°$
$h = -8 \rightarrow 8$
$k = -25 \rightarrow 25$
$l = -10 \rightarrow 10$

Refinement

Refinement on F^2
Least-squares matrix: full
$R[F^2 > 2\sigma(F^2)] = 0.038$
$wR(F^2) = 0.106$
$S = 1.04$
2362 reflections
193 parameters
0 restraints

Hydrogen site location: mixed
H atoms treated by a mixture of independent and constrained refinement
$w = 1/[\sigma^2(F_o^2) + (0.0576P)^2 + 0.4126P]$ where $P = (F_o^2 + 2F_c^2)/3$
$(\Delta/\sigma)_{\max} = 0.019$
$\Delta\rho_{\max} = 0.18$ e Å^{-3}
$\Delta\rho_{\min} = -0.25$ e Å^{-3}

Special details

Geometry. All esds (except the esd in the dihedral angle between two l.s. planes) are estimated using the full covariance matrix. The cell esds are taken into account individually in the estimation of esds in distances, angles and torsion angles; correlations between esds in cell parameters are only used when they are defined by crystal symmetry. An approximate (isotropic) treatment of cell esds is used for estimating esds involving l.s. planes.

Fractional atomic coordinates and isotropic or equivalent isotropic displacement parameters (Å²)

	x	*y*	*z*	U_{iso}*/U_{eq}
O1	0.20414 (13)	0.21597 (5)	0.52257 (12)	0.0216 (3)
H1	0.248 (2)	0.2057 (8)	0.616 (2)	0.032*
N1	0.37839 (14)	0.30976 (5)	0.32442 (13)	0.0152 (3)
C1	0.32460 (18)	0.19901 (6)	0.40609 (16)	0.0171 (3)
H1A	0.256590	0.191054	0.306579	0.020*
H1B	0.385335	0.159619	0.437830	0.020*
C2	0.46484 (18)	0.25029 (6)	0.38038 (16)	0.0164 (3)
H2A	0.534355	0.258221	0.479141	0.020*
H2B	0.546544	0.235486	0.302886	0.020*
C3	0.38451 (17)	0.35642 (6)	0.42167 (15)	0.0146 (3)
H3	0.444841	0.350163	0.519987	0.017*
C4	0.30263 (16)	0.41963 (6)	0.38920 (15)	0.0130 (3)
C5	0.23407 (17)	0.43504 (6)	0.23570 (15)	0.0145 (3)
H5	0.237547	0.404567	0.155754	0.017*
C6	0.16132 (16)	0.49467 (6)	0.20070 (15)	0.0143 (3)
H6	0.117589	0.503528	0.097642	0.017*
C7	0.15235 (16)	0.54192 (6)	0.31769 (15)	0.0128 (3)
C8	0.07710 (17)	0.60437 (6)	0.28453 (15)	0.0154 (3)
H8	0.035518	0.614331	0.181508	0.019*
C9	0.06565 (17)	0.64883 (6)	0.40009 (16)	0.0167 (3)
H9	0.016214	0.688652	0.375061	0.020*
C10	0.12884 (16)	0.63543 (6)	0.56126 (15)	0.0140 (3)
C11	0.11339 (17)	0.68037 (6)	0.68337 (17)	0.0174 (3)
H11	0.060084	0.719801	0.660935	0.021*
C12	0.17704 (17)	0.66639 (6)	0.83720 (16)	0.0179 (3)
H12	0.166897	0.696676	0.916797	0.021*
C13	0.25590 (17)	0.60745 (6)	0.87342 (15)	0.0167 (3)
H13	0.299764	0.599066	0.976686	0.020*
C14	0.27000 (16)	0.56069 (6)	0.75641 (15)	0.0138 (3)
C15	0.34525 (17)	0.49843 (6)	0.78892 (15)	0.0149 (3)
H15	0.386896	0.488566	0.891982	0.018*
C16	0.35730 (17)	0.45384 (6)	0.67445 (15)	0.0146 (3)
H16	0.407480	0.414277	0.701019	0.018*
C17	0.29455 (16)	0.46569 (6)	0.51163 (15)	0.0125 (3)
C18	0.21810 (16)	0.52728 (6)	0.47568 (15)	0.0122 (3)
C19	0.20622 (16)	0.57444 (6)	0.59733 (15)	0.0126 (3)

Atomic displacement parameters (Å^2)

	U^{11}	U^{22}	U^{33}	U^{12}	U^{13}	U^{23}
O1	0.0190 (5)	0.0258 (6)	0.0203 (5)	0.0037 (4)	0.0046 (4)	0.0078 (4)
N1	0.0156 (6)	0.0122 (6)	0.0180 (6)	−0.0018 (4)	0.0029 (4)	0.0010 (4)
C1	0.0208 (7)	0.0129 (7)	0.0173 (7)	0.0002 (5)	−0.0013 (5)	0.0012 (5)
C2	0.0168 (7)	0.0151 (7)	0.0175 (7)	0.0025 (5)	0.0021 (5)	−0.0003 (5)
C3	0.0127 (6)	0.0167 (7)	0.0145 (6)	−0.0029 (5)	0.0020 (5)	0.0011 (5)
C4	0.0098 (6)	0.0138 (7)	0.0156 (7)	−0.0029 (5)	0.0022 (5)	0.0017 (5)
C5	0.0141 (7)	0.0148 (7)	0.0150 (7)	−0.0027 (5)	0.0028 (5)	−0.0022 (5)
C6	0.0119 (6)	0.0191 (7)	0.0118 (6)	−0.0016 (5)	−0.0009 (5)	0.0029 (5)
C7	0.0086 (6)	0.0162 (6)	0.0139 (6)	−0.0028 (5)	0.0020 (5)	0.0024 (5)
C8	0.0129 (6)	0.0187 (7)	0.0146 (6)	−0.0001 (5)	0.0001 (5)	0.0049 (5)
C9	0.0131 (6)	0.0135 (6)	0.0235 (7)	0.0007 (5)	0.0020 (5)	0.0054 (5)
C10	0.0099 (6)	0.0143 (7)	0.0181 (7)	−0.0030 (5)	0.0030 (5)	0.0001 (5)
C11	0.0129 (6)	0.0146 (7)	0.0248 (8)	−0.0007 (5)	0.0031 (5)	−0.0008 (5)
C12	0.0156 (7)	0.0174 (7)	0.0209 (7)	−0.0036 (5)	0.0039 (5)	−0.0063 (6)
C13	0.0142 (7)	0.0227 (7)	0.0134 (7)	−0.0049 (5)	0.0015 (5)	−0.0014 (5)
C14	0.0093 (6)	0.0160 (7)	0.0162 (7)	−0.0039 (5)	0.0023 (5)	0.0004 (5)
C15	0.0127 (6)	0.0198 (7)	0.0119 (6)	−0.0026 (5)	−0.0006 (5)	0.0022 (5)
C16	0.0135 (6)	0.0129 (6)	0.0173 (7)	−0.0003 (5)	0.0001 (5)	0.0043 (5)
C17	0.0093 (6)	0.0138 (7)	0.0144 (6)	−0.0036 (5)	0.0021 (5)	0.0018 (5)
C18	0.0079 (6)	0.0144 (7)	0.0146 (7)	−0.0034 (5)	0.0023 (5)	0.0014 (5)
C19	0.0082 (6)	0.0155 (7)	0.0143 (7)	−0.0036 (5)	0.0031 (5)	0.0002 (5)

Geometric parameters (Å, º)

O1—C1	1.4148 (17)	C8—H8	0.9300
O1—H1	0.862 (19)	C9—C10	1.4415 (19)
N1—C3	1.2745 (17)	C9—H9	0.9300
N1—C2	1.4662 (17)	C10—C11	1.4051 (19)
C1—C2	1.5215 (19)	C10—C19	1.4254 (19)
C1—H1A	0.9700	C11—C12	1.388 (2)
C1—H1B	0.9700	C11—H11	0.9300
C2—H2A	0.9700	C12—C13	1.3918 (19)
C2—H2B	0.9700	C12—H12	0.9300
C3—C4	1.4750 (18)	C13—C14	1.3988 (19)
C3—H3	0.9300	C13—H13	0.9300
C4—C5	1.4029 (19)	C14—C19	1.4279 (19)
C4—C17	1.4171 (19)	C14—C15	1.4378 (19)
C5—C6	1.3847 (19)	C15—C16	1.3500 (19)
C5—H5	0.9300	C15—H15	0.9300
C6—C7	1.4019 (19)	C16—C17	1.4476 (18)
C6—H6	0.9300	C16—H16	0.9300
C7—C18	1.4275 (18)	C17—C18	1.4337 (19)
C7—C8	1.4424 (18)	C18—C19	1.4307 (19)
C8—C9	1.3543 (19)		

O1···N1	2.9300 (19)	H1···C2^{i}	2.841 (16)
O1···N1^{i}	2.8440 (18)	C3···H16	2.65
N1···H5	2.62	C16···H3	2.63
H1···N1^{i}	1.997 (16)	H1···H5^{i}	2.33
C3···C19^{ii}	3.386 (2)	H2A···H3	2.07
C17···C17^{ii}	3.396 (2)	H3···H16	2.06

C1—O1—H1	110.7 (12)	C8—C9—H9	119.5
C3—N1—C2	116.32 (11)	C10—C9—H9	119.5
O1—C1—C2	113.01 (11)	C11—C10—C19	119.43 (12)
O1—C1—H1A	109.0	C11—C10—C9	121.79 (12)
C2—C1—H1A	109.0	C19—C10—C9	118.78 (12)
O1—C1—H1B	109.0	C12—C11—C10	120.53 (13)
C2—C1—H1B	109.0	C12—C11—H11	119.7
H1A—C1—H1B	107.8	C10—C11—H11	119.7
N1—C2—C1	110.61 (11)	C11—C12—C13	120.60 (12)
N1—C2—H2A	109.5	C11—C12—H12	119.7
C1—C2—H2A	109.5	C13—C12—H12	119.7
N1—C2—H2B	109.5	C12—C13—C14	120.81 (12)
C1—C2—H2B	109.5	C12—C13—H13	119.6
H2A—C2—H2B	108.1	C14—C13—H13	119.6
N1—C3—C4	124.59 (12)	C13—C14—C19	119.30 (12)
N1—C3—H3	117.7	C13—C14—C15	122.89 (12)
C4—C3—H3	117.7	C19—C14—C15	117.82 (12)
C5—C4—C17	119.30 (12)	C16—C15—C14	122.03 (12)
C5—C4—C3	120.13 (12)	C16—C15—H15	119.0
C17—C4—C3	120.56 (12)	C14—C15—H15	119.0
C6—C5—C4	121.40 (12)	C15—C16—C17	122.05 (12)
C6—C5—H5	119.3	C15—C16—H16	119.0
C4—C5—H5	119.3	C17—C16—H16	119.0
C5—C6—C7	121.24 (12)	C4—C17—C18	119.31 (12)
C5—C6—H6	119.4	C4—C17—C16	123.47 (12)
C7—C6—H6	119.4	C18—C17—C16	117.21 (12)
C6—C7—C18	118.67 (12)	C7—C18—C19	119.41 (12)
C6—C7—C8	122.39 (12)	C7—C18—C17	120.07 (12)
C18—C7—C8	118.94 (12)	C19—C18—C17	120.52 (12)
C9—C8—C7	121.47 (12)	C10—C19—C14	119.31 (12)
C9—C8—H8	119.3	C10—C19—C18	120.32 (12)
C7—C8—H8	119.3	C14—C19—C18	120.38 (12)
C8—C9—C10	121.07 (12)		

C3—N1—C2—C1	110.27 (13)	C3—C4—C17—C18	178.50 (10)
O1—C1—C2—N1	−61.54 (14)	C5—C4—C17—C16	178.35 (11)
C2—N1—C3—C4	−178.71 (11)	C3—C4—C17—C16	−2.55 (19)
N1—C3—C4—C5	−9.67 (19)	C15—C16—C17—C4	−178.97 (12)
N1—C3—C4—C17	171.23 (12)	C15—C16—C17—C18	0.00 (18)
C17—C4—C5—C6	1.06 (19)	C6—C7—C18—C19	−178.58 (11)
C3—C4—C5—C6	−178.05 (11)	C8—C7—C18—C19	0.64 (17)

C4—C5—C6—C7	−0.38 (19)	C6—C7—C18—C17	1.17 (17)
C5—C6—C7—C18	−0.74 (18)	C8—C7—C18—C17	−179.62 (11)
C5—C6—C7—C8	−179.92 (11)	C4—C17—C18—C7	−0.50 (18)
C6—C7—C8—C9	178.35 (12)	C16—C17—C18—C7	−179.52 (10)
C18—C7—C8—C9	−0.83 (18)	C4—C17—C18—C19	179.24 (10)
C7—C8—C9—C10	0.13 (19)	C16—C17—C18—C19	0.23 (18)
C8—C9—C10—C11	−178.20 (12)	C11—C10—C19—C14	−1.30 (18)
C8—C9—C10—C19	0.74 (18)	C9—C10—C19—C14	179.74 (11)
C19—C10—C11—C12	1.71 (19)	C11—C10—C19—C18	178.05 (11)
C9—C10—C11—C12	−179.36 (12)	C9—C10—C19—C18	−0.91 (18)
C10—C11—C12—C13	−0.53 (19)	C13—C14—C19—C10	−0.27 (18)
C11—C12—C13—C14	−1.1 (2)	C15—C14—C19—C10	179.26 (11)
C12—C13—C14—C19	1.47 (19)	C13—C14—C19—C18	−179.61 (11)
C12—C13—C14—C15	−178.03 (11)	C15—C14—C19—C18	−0.09 (17)
C13—C14—C15—C16	179.82 (12)	C7—C18—C19—C10	0.23 (18)
C19—C14—C15—C16	0.32 (18)	C17—C18—C19—C10	−179.52 (11)
C14—C15—C16—C17	−0.28 (19)	C7—C18—C19—C14	179.57 (11)
C5—C4—C17—C18	−0.61 (18)	C17—C18—C19—C14	−0.18 (18)

Symmetry codes: (i) *x*, −*y*+1/2, *z*+1/2; (ii) −*x*+1, −*y*+1, −*z*+1.

Hydrogen-bond geometry (Å, º)

D—H···*A*	*D*—H	H···*A*	*D*···*A*	*D*—H···*A*
O1—H1···N1^{i}	0.853 (17)	1.997 (16)	2.8440 (18)	171.6 (14)

Symmetry code: (i) *x*, −*y*+1/2, *z*+1/2.